Removal of Oil Films from Stainless Steel Tubes

Jenn-Feng Yan, A. Eduardo Sáez and Christine S. Grant
Dept. of Chemical Engineering, North Carolina State University, Raleigh, NC 27695

The removal of oil films from the inner surface of a stainless steel tube cell using aqueous cleaning solutions was studied. The two oils used in the cleaning experiments, Sunquench 1042 and heavy mineral oil, contained P^{32} labeled tributyl phosphate (TBP) as a radioactive tracer. The β^- particles emitted from the radioactive TBP were detected by a CaF_2 scintillator and used as a measure of the amount of oil remaining in the tube cell. Cleaning experiments performed at different flow rates, surface treatment, and surfactant concentrations indicated that initially the oil films were removed rapidly. At the end of the experiments, the oil removal rate reduced significantly, eventually becoming negligible. The stainless steel morphology affected oil removal significantly, and the rougher tube tended to retard the oil removal. The rate and extent of the decontamination were significantly increased in the presence of sodium dodecyl sulfate, a nonionic surfactant. Experimental data were compared to a hydrodynamic model based on the removal of a liquid contaminant from a solid surface by an immiscible fluid. The model deviated from the experimental data due to the presence of instabilities at the oil-water interface.

Introduction

The contamination of metal surfaces with oil is a widespread problem in the chemical, metalworking, and automotive industries. The main source of oil fouling comes from the process fluids in various operations. For example, in a heat exchanger, the oil contaminates the equipment surface causing a lower heat-transfer efficiency. The fouled equipment leads to increased costs due to added heat-transfer area, maintenance, energy, and production losses caused by unit downtime.

In the auto industry and in military installations a large fraction of oil fouling is from lubricants. The primary functions of lubricants are: (1) to reduce the friction and wear in the moving parts of a machine; (2) to be used as heat-transfer media; (3) to protect machine parts against corrosion; and (4) to act as carriers for solid contaminants (Royal Dutch/Shell Group, 1983). A desirable property of the lubricant is its capacity to adhere tightly to metal surfaces. The dominant source of lubricants is mineral oil which is derived from crude petroleum. Synthetic lubricants and fatty oils derived from animal or vegetable fats are also used. Fatty oils, which are very strongly adsorbed onto metals, are often blended with minerals to form compound oils. ASTM defines a grease as a solid to semi-fluid product of a thickening agent (such as metallic soap) in a liquid lubricant (such as petroleum oil). Greases are often used when the parts being lubricated are inaccessible, inadequately sealed, or there is a danger of the oil contaminating the product. The consistency of the grease depends on the nature of the thickener added to the oil; typical thickeners include calcium, lithium, or other organics. Cleaning processes are needed for removing these contaminant oils and greases from metal surfaces.

Another application of cleaning techniques in the auto industry is the recycling and reuse of vehicles and automotive components. Approximately 94% of U.S. cars and trucks are currently returned to dismantling and shredding facilities (Materials Performance, 1994). Of that total, 75% of the vehicle's content is recycled, including automotive components which are in contact with oil and need to be cleaned before reuse.

Cleaning in place (CIP) techniques minimize the requirements of time, labor, cleaning solvent, and energy associated with the disassembling of process equipment (Wennerberg, 1981). CIP has been utilized for over 30 years in the food and dairy processing industry and for almost 10 years in pharmaceutical plants. In the last few years various sectors of the chemical industry have been incorporating CIP into their processes (Chowchury and Ondrey, 1994). When CIP techniques are used, it is hard to monitor the rate at which the

Correspondence concerning this article should be addressed to C. S. Grant.
Current address of J.-F. Yan: Phillips Components, Columbia, SC 29212.

surface is being cleaned and verify the cleanliness of the internal surface. The aforementioned uncertainty results in the inefficient use of cleaning reagents (such as surfactant) and decontamination solvents (such as acid). This leads to a higher material expense and an associated cost for the separation and recovery of the cleaning reagents and decontamination solvents. Despite the importance of oil fouling and cleaning in the above industries, very little attention has been paid to fundamental studies of oil decontamination mechanisms. The development of environmentally benign cleaning processes requires an understanding of the fundamental mechanisms governing the adhesion and removal of residues.

In a typical cleaning experiment, an evaluation is made of the amount of contaminant remaining on the surface or removed from the solid substrate. The determination of remaining contaminant after cleaning may include: a direct measurement of the amount left on the surface, or an assessment of a physical property of the surface related to the amount of contaminant remaining (Corrieu, 1981; Jennings, 1963; Kulkarni et al., 1975; Plett, 1985). The amount of contaminant removed may be determined by analyzing the effluent (Perka et al., 1993). The main limitation to these techniques is that the experiments are often either discontinuous or invasive in nature.

Mickaily and Middleman (1993) recently presented the results of a gravimetric cleaning study in which air was used as a flushant to remove oil from small (0.4–0.6 cm dia.) aluminum capillary tubes. Their study was motivated by the need to develop a solventless cleaning process as an alternative to current environmentally detrimental solvents (such as trichloroethane). They developed a hydrodynamic model to describe the decontamination process and reported that the flushing action of an immiscible fluid can result in low levels of residual oils; the removal in this case was due only to the hydrodynamic shear of the air. They observed that the surface roughness limits the rate and extent of the hydrodynamic cleaning process.

In the work described here, an on-line solid scintillation technique has been developed to continuously and noninvasively evaluate the amount of contaminant remaining on the inner surface of metal tubes. The rate of contaminant removal is studied in the region of fully developed turbulent flow corresponding to the majority of industrial cleaning operations. The radioactive signal from the contaminant on the inner surface of the flow cell is detected at the outer surface by standard scintillation devices and processed electronically to indicate the amount of contaminant remaining as a function of time. The removable flow cell allows control of both the application of the film and the analysis of the cell after decontamination. The technique has been successfully used to study the removal of calcium phosphate residues from stainless steel tubes (Grant et al., 1996).

Experimental Procedure

Materials

Two oils were used in the cleaning experiments reported in this article: Sunquench 1042 (provided by Dow Chemical Co.) and heavy mineral oil (Fisher Scientific, $\geq 59\%$ purity). Tributyl phosphate (TBP, Fisher Scientific, 99%), irradiated in the nuclear reactor (Pulstar Light Water) at North Carolina State University, was added to the oils as a radioactive tracer in the decontamination tests. Radioactive TBP contains the P^{32} isotope and produces β^- particles with a half-life of 14 days. A ten-to-one oil to TBP volume ratio was used to coat the inner surface of the tube cell. The viscosities of the oil/TBP mixtures were measured using a dynamic stress rheometer (Rheometrics Inc., Model DSR 100). The densities of the resulting mixtures were predicted from the volume fractions of the oil and TBP. The measured viscosities and densities at 20°C are listed in Table 1.

Table 1. Properties of Oils and Oil/TBP Mixtures at 20°C

	μ (cp)	ρ (g/cm^3)
Sunquench	292	0.89
Sunquench + TBP	132	0.898
Mineral oil (heavy)	127	0.87
Mineral oil (heavy) + TBP	64	0.88

The initial cleaning solution was water obtained from a reverse osmosis (RO) unit (Culligan, Model RS2). The solution temperature, conductivity, and pH were measured to be 17–21°C, 65–75 μS/cm, and 6.7–6.9 respectively. Nonionic surfactant solutions (2.4×10^{-3} M and 4.8×10^{-3} M) were prepared by dissolving sodium dodecyl sulfate (SDS, Fisher Scientific) in RO water. These SDS concentrations are below the reported critical micelle concentration (CMC) of the surfactant in water (8.0×10^{-3} M) (van Os et al., 1993).

Experimental apparatus

Flow System. The flow system and the tube cell are shown in Figure 1. The system was composed of a cleaning solution storage tank (180 L), a micropump (Micropump Model 101-415), a flowmeter (Omega), a stainless steel (SS304) tube cell, and stainless steel (SS304) piping. The solvent is pumped through the experimental flow system to remove the oil film and returned to the tank for recycle. The solvent flow rate was controlled in a range of 3.59 to 9.94 L/min, which is equivalent to a range of Reynolds numbers from 7,257 to 20,091. The stainless steel tube cells were fabricated by the Precision Engineering Shop at North Carolina State University. To allow a high rate of transmission of β^- particles, the tube cell has a thin window which is 0.102 mm in thickness. The window accounts for 7.5% of the total tube surface area and was positioned against the CaF_2 scintillator detector during the decontamination tests. The tube cell was 60 mm in length and its OD was 12.7 mm. The ID of the tube cell is 10.5 mm which is equal to that of the connecting piping. In addition, there is a 100-cm-long pipe prior to the tube cell to ensure well-developed turbulent flow before water enters the tube cell. The window was 20 mm in length and it was centered with respect to the length of the tube cell. This left 20 mm of tube cell before and after the scintillation window.

In order to investigate the role of surface morphology on the cleaning process, tube cells were created with three different surface roughness values: No. 4, No. 32, and No. 63 finish. A Form Talysurf Stylus profilometer was used to perform roughness measurements on stainless steel coupons that were prepared using the same technique as the inner surface of the tube cell. The roughness measurements were reported in terms of a root mean square value (R_q). This represents

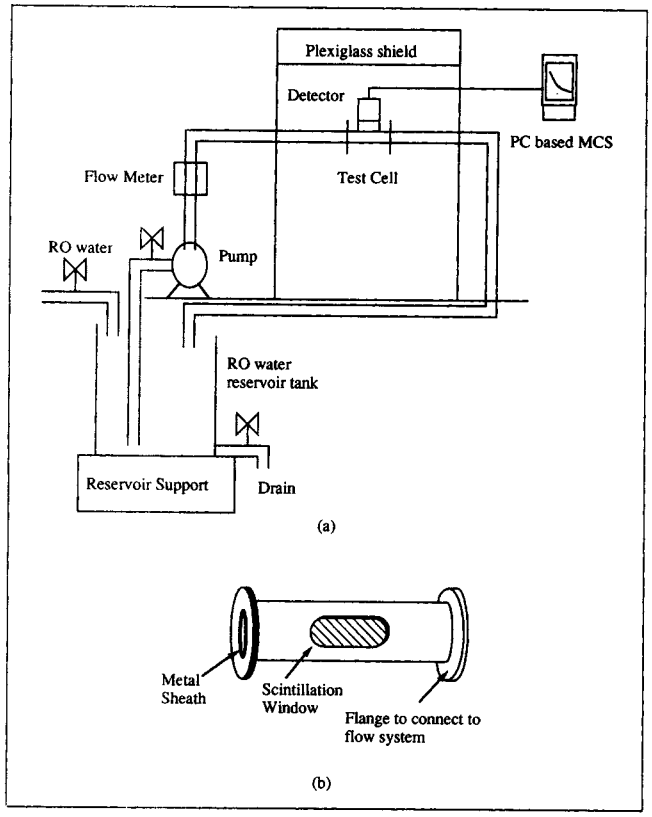

Figure 1. (a) Experimental flow system; (b) tube cell.

the average distance from the mean line for the peaks and the valleys in the substrate. The average depth of the surface cavities (δ_{avg}) is approximately two times the R_q values assuming a skewness (R_{sk}) value of zero. The arithmetric average of the depth of these three surface roughnesses (measured and ideal) and the range of the skewness for each roughness are listed in Table 2. The ideal values are based on the number of the surface finish.

Detection System. Figure 2 shows a block diagram of the associated electronics in the solid scintillation detection system. The scintillation detector positioned on the outside of the tube cell takes measurements of β^- emission continuously without disturbing the flow field in the tube cell. The β^- emission corresponds to a measure of the amount of contaminant remaining in the tube cell. The CaF_2 scintillation detector (Bicron) was selected due to its high β^- efficiency and its capability for spectroscopy (Tsoulfanidis, 1983). The light signal from the CaF_2 scintillation detector is sent to a photomultiplier tube (Bicron) where it is amplified and converted to an electronic signal. This signal is transmitted through a preamplifier (Tennelec TC145), an amplifier (Tennelec TC241), and a multichannel scalar (Oxford). The multichannel scalar converts the raw signal to net emission counts. These signals are sent in digital form to an IBM-compatible personal computer which displays and stores the signals for future analysis.

Table 2. Morphology of Stainless Steel Tube Cells

Surface Finish	δ_{avg} (μin) (Ideal)	δ_{avg} (cm) (Ideal)	Measured δ_{avg} (cm) Avg. of 3 Meas. $2\times R_q$	R_{sk} Range
No. 4	4	1.02×10^{-5}	3.9×10^{-5}	(−0.6)–(0.16)
No. 32	32	8.16×10^{-5}	9.0×10^{-5}	(−0.56)–(−0.33)
No. 63	63	1.60×10^{-4}	2.0×10^{-4}	(−0.95)–(−0.51)

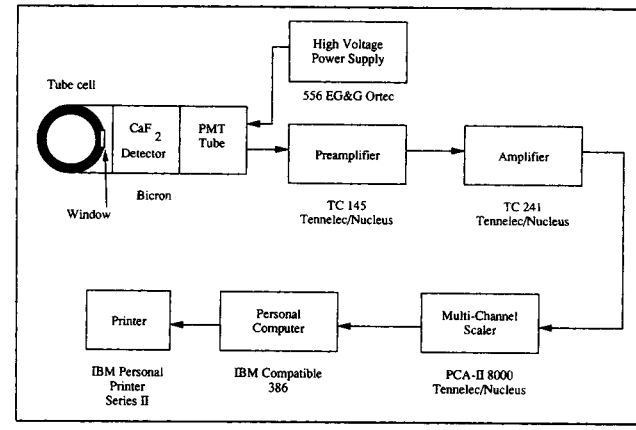

Figure 2. Electronics of the solid scintillation detection system.

Oil coating and decontamination experiments

The mixture used to coat the cell consisted of oil, TBP, and toluene. Toluene was added to the oil/TBP mixture to reduce the viscosity of the mixture so that it could easily flow in the tube cell during the coating process. A oil/TBP film tilted rotational coating technique was developed using glass tubes and dyed oil mixtures; a three-to-one toluene to oil ratio was found to produce the most uniform coatings. A fixed amount of the oil mixture was placed into the tube cell mounted on the top of a tilted rotator. The tube cell was rotated at 30 rpm; the angle of the rotator was changed every 30 s to reverse the flow of the mixture. After 5 min the cell was rotated in a horizontal position for 30 min at 90°C under a UV lamp to evaporate the toluene. The initial mass of the oil/TBP in the tube cell was determined gravimetrically. The oil/TBP film thickness was determined from the composition of the mixture (i.e., the oil/TBP ratio and the oil/solvent ratio) and the volume of the mixture placed in the tube cell. A typical volume of the mixture was 100 μL, which results in an oil film thickness of 10 μm, assuming complete evaporation of the toluene.

The tube cell was inserted into the flow apparatus and tightened with C-clamps at both ends. The window was positioned against the scintillation detector; before the flow was started, the activity of the coating was measured for 2 min. The pump was turned on and the net β^- counts over the entire emission spectrum were measured in 10-s intervals.

Interpretation of scintillation data

The net counts detected by the solid scintillator were assumed to correspond to the oil/TBP film in the tube cell. However, two items need to be considered before analyzing the raw scintillation data: the background counts and the water dampening effect. The background counts due to environmental lighting (such as fluorescence room lighting) were de-

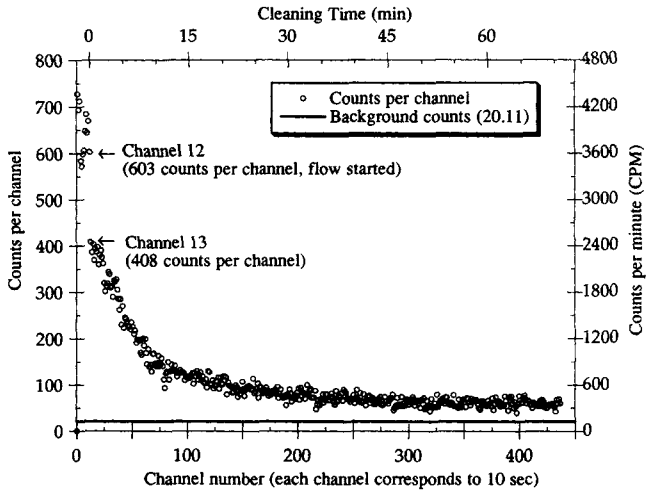

Figure 3. Example of raw data from solid scintillation (Sunquench, No. 32 cell, fresh water, 3.59 L/min, single coating).

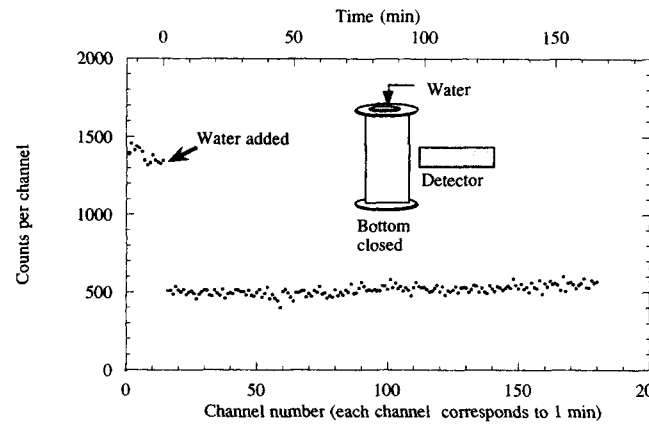

Figure 4. Dampening effect of water in the solid scintillation system (No. 4 cell, no flow, fresh water, Sunquench, single coating).

termined before each test by measuring the counts from the uncoated tube cell. The net counts due to the oil/TBP coating were obtained by subtracting the background counts from the total emission from a coated cell. Figure 3 presents the typical raw scintillation data as the total counts per channel versus the channel number for a single coating of Sunquench oil in a No. 32 tube cell. Each channel represents a 10-s count over the entire emission spectrum of the P^{32}. This data can also be presented as the total counts per minute (CPM) as shown in the right side of y-axis in Figure 3. In a given cleaning experiment, the background counts are a small fraction of the raw scintillation data.

The first 12 data points in Figure 3 correspond to the activity of the coating during the first 2 min of the experiment in the absence of water in the cell. When the tube cell was initially filled with water, there was an abrupt drop in the signal (from 603 to 408 CPM in Figure 3). This drop was because water, a low density material, absorbs the energy of β^- particles and substantially reduces the emission counts when the cell is filled with water. An experiment was performed to measure the signal dampening associated with the presence of the solvent. In this experiment, there was a sudden decrease in the signal, when 10 mL of RO water was slowly poured into a coated tube cell maintained in a vertical position as shown in Figure 4. In this experiment, because there was essentially no water flow in the system, it was verified that the sudden drop was due to the dampening of the water and not the initial removal of copious oil/TBP from the tube surface. To account for the dampening effect, the data collected during decontamination experiments have been normalized to the signal strength after 10 s of water flow. In Figure 3, the upper x-axis represents the decontamination time after the signal is converted due to the water dampening effect.

The raw scintillation data exhibits a great deal of scatter at long times especially towards the end of the experiment when the counts are low. This scatter is due to the statistical error associated with radioactive emissions, which are stochastic events (Tsoulfanidis, 1983).

Theory

In this section we propose a model to predict the thinning rate of the viscous film deposited on the inner surface of the tube. The model proposed is a modification of the development presented by Mickaily and Middleman (1993). We will consider that the viscous film is constantly sheared by a flushant fluid that occupies the core of the pipe which is in the turbulent flow regime (Figure 5). We will assume that the film thickness always satisfies $H \ll R$. The flushant fluid is immiscible with the fluid in the film, and its motion causes a shear flow in the film.

A mass balance on a differential section of the film leads to a governing equation for changes in film thickness (H),

$$\frac{\partial H}{\partial t} + \frac{\partial q}{\partial z} = 0 \tag{1}$$

where q is the oil volume flow rate per unit film width.

The flushant liquid exerts a shear stress τ_0 on the film surface in the direction of flow. This shear stress will be considered to be constant and uniform along the test cell, and it

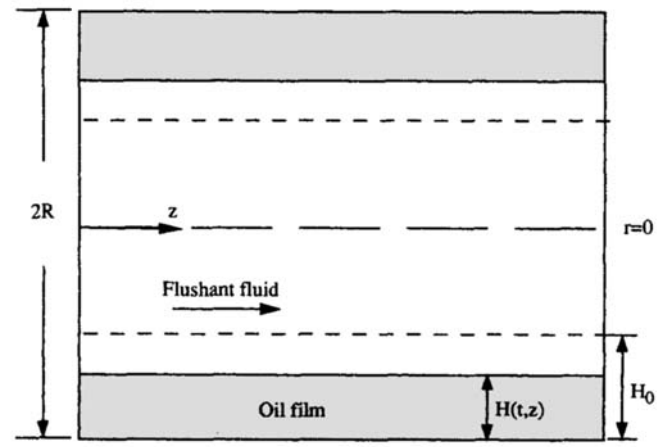

Figure 5. Hydrodynamic model.

can be evaluated from the Fanning friction factor (f) by means of

$$\tau_0 = \frac{1}{2} f \rho \left(\frac{Q}{\pi R^2} \right)^2 \tag{2}$$

where ρ is the flushant density, Q is the flushant flow rate, and R is the tube radius. The friction factor can be obtained from a standard f vs. Reynolds number plot (see, for example, Geankopolis, 1993). For this purpose, we will assume that the surface of the film can be considered a smooth wall.

If the variations of film thickness with z (axial coordinate) are considered to be small, as in the standard lubrication approximation, then the velocity profile within the film is linear with radial position and the film mean velocity (V) can be related to the shear stress by

$$V = \frac{H\tau_0}{2\mu_{oil}} \tag{3}$$

where μ_{oil} is the viscosity of the film. Furthermore, since $q = VH$, using Eq. 3, Eq. 1 becomes

$$\frac{\partial H}{\partial t} + \frac{H\tau_0}{\mu_{oil}} \frac{\partial H}{\partial z} = 0 \tag{4}$$

This differential equation will be expressed in dimensionless form by defining the following dimensionless variables: $h = H/H_0$, where H_0 is the initial film thickness, $\xi = z/L$, where L is the length of the test cell, and θ (dimensionless flushing time) $= t/t_c$, where

$$t_c = \frac{\mu_{oil} L}{\tau_0 H_0} \tag{5}$$

The resulting equation is

$$\frac{\partial h}{\partial \theta} + h \frac{\partial h}{\partial \xi} = 0 \tag{6}$$

with initial condition $h = 1$ when $\theta = 0$.

Equation 6 can be solved by the method of characteristics. The total differential of $h(\theta, \xi)$ is

$$dh = \frac{\partial h}{\partial \theta} d\theta + \frac{\partial h}{\partial \xi} d\xi \tag{7}$$

A direct comparison of Eqs. 6 and 7 reveals that a line $\xi = \xi_h(\theta)$ on which h is a constant satisfies

$$\frac{d\xi_h}{d\theta} = h \tag{8}$$

which leads to

$$\xi_h = h\theta + \xi_{h0} \tag{9}$$

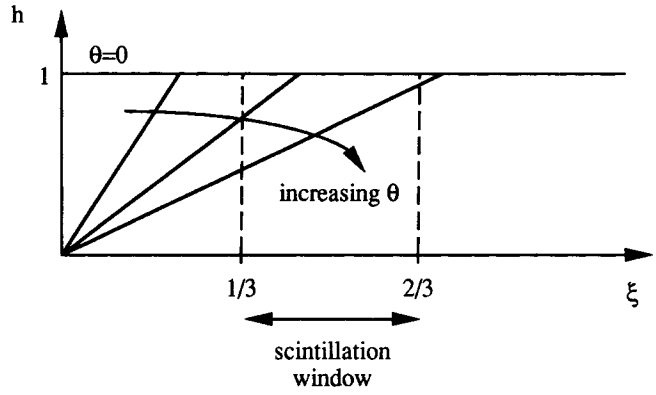

Figure 6. Evolution of film thickness according to the hydrodynamic model.

where ξ_{h0} is the dimensionless axial location of a point with film thickness h at $\theta = 0$. Since the film starts as a discontinuity at $\xi = 0$, the location at $\theta = 0$ of all possible values of h ($0 \le h \le 1$) is $\xi_{h0} = 0$. Therefore, the characteristic curve is $\xi_h = h\theta$. This means that, at a given dimensionless time θ, h is a linear function of ξ that starts at $h = 0$. Therefore, at a given θ, the film thickness increases with ξ until the original thickness is reached ($h = 1$). This point marks the perturbation front that advances downstream as time passes. The evolution of film morphology according to this solution is shown in Figure 6.

The general solution for a given θ is then given by

$$h = \frac{\xi}{\theta} \qquad 0 \le \xi \le \theta$$
$$h = 1 \qquad \theta < \xi \tag{10}$$

Note that the solution presented implicitly assumes that the contact line formed at the upstream end of the film ($\xi = 0$) does not move while the film thins. This might be too strong an assumption, but a motion of the contact line would presumably lead to faster cleaning so that our solution could be interpreted as the lower bound on cleaning rates, i.e., an upper bound on average film thickness.

Mickaily and Middleman (1993) developed a model for the problem considered here by starting from the same basic equations, but they disregarded the solution by the method of characteristics and went on to develop an equation for the average film thickness. In their development they make the assumption that the film thickness is uniform which, as they point out, is inconsistent with the basic differential Eq. 1. They arrive at a final equation that gives film thickness as a function of time and then modify it empirically to fit experimental data. In this work we will use the solution developed by the method of characteristics as a basis of comparison of cleaning rates with experimental observations.

In our experiments we measured the fraction of oil removal within the length of the scintillation window. The amount of oil removed is related to the average film thickness in that region, which comprises the range $1/3 < \xi < 2/3$. The average dimensionless thickness can be calculated by

$$\bar{h} = 3\int_{1/3}^{2/3} h\,d\xi \tag{11}$$

By using Eq. 10, the average thickness can be obtained as a function of dimensionless time, which yields

$$\begin{aligned} \bar{h} &= 1 && 0 \le \theta \le 1/3 \\ \bar{h} &= 2 - \frac{1}{2}\left(3\theta + \frac{1}{3\theta}\right) && 1/3 < \theta \le 2/3 \\ \bar{h} &= \frac{1}{2\theta} && 2/3 < \theta \end{aligned} \tag{12}$$

where $\bar{h}$ is dimensionless average film thickness. This equation predicts, as expected, that the film becomes continuously thinner until all the oil is removed (as $\theta \to \infty$). As will be clear below, our results indicate that this is not the case. We have found that a residual amount of oil remains on the wall at long times. To account for this, we will assume that this residual oil is not affected at any time by the shear flow, i.e., we will consider that a certain volume of the original oil in the scintillation window V_c remains inaccessible during the cleaning process, by accumulating in the rough portions of the tube. The ratio between V_c and the original oil in the film within the portion of the tube measured in the scintillation window is given by

$$\alpha = \frac{V_c}{2\pi R L_c H_0} \tag{13}$$

where L_c is the length of the scintillation window ($L_c = 20$ mm) and V_c is inaccessible film volume. Note that this parameter represents the fractional amount of oil, relative to the original film, that is not removed in the cleaning process.

The fraction of oil remaining in the cell at a given time ϵ can be expressed in terms of the residual oil as

$$\epsilon = \frac{\bar{h} + \alpha}{1 + \alpha} \tag{14}$$

By combining Eqs. 12 and 14, we can predict the amount of oil remaining as a function of time, once α is known. The fractional residual oil can be determined from the experimental data by determining the asymptotic value, as $t \to \infty$, of the fraction of oil remaining (ϵ_∞) from the equation

$$\epsilon_\infty = \frac{\alpha}{1 + \alpha} \tag{15}$$

Results and Discussion

Because the half-life of a P^{32} isotope is only 14 days, it was inappropriate to use the absolute counts to represent the amount of oil removed. Instead, all scintillation data were presented as the fraction of oil remaining, determined from

$$\epsilon = \frac{C_i}{C_0} \tag{15}$$

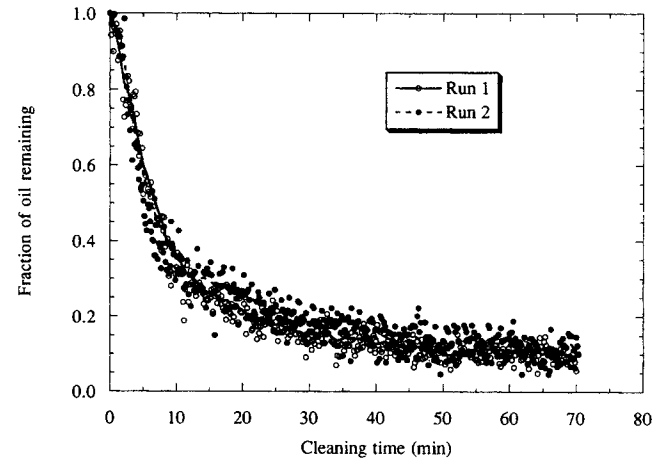

Figure 7. Reproducibility of decontamination runs (3.59 L/min, No. 32 cell, single coating, Sunquench).

where C_0 is the initial net counts and C_i the net counts at time i with the modifications due to the dampening effect of the water and the background light.

Figure 7 shows a typical result of a decontamination test after normalizing the raw data (from Figure 3) to the initial net counts. It also indicates the reproducibility of the solid scintillation technique. At longer experimental times, there are more than 2,000 data points collected in each experiment. In order to present several sets of data and compare the experimental data to the theory, in the rest of the figures the data will be presented as smoothed curves rather than as individual data points.

Figure 8 shows the removal of Sunquench oil films from a No. 63 cell at different flow rates, along with the model predictions. The cleaning curves exhibit a fast cleaning rate at short times, followed by slower cleaning at long times until a residual amount of oil remains at the end of the cleaning process. This residual amount decreases as the flushant flow rate is increased. Presumably, the oil film breaks at one point during the cleaning and a residual amount is trapped by the cavities that constitute the roughness of the tube wall. This

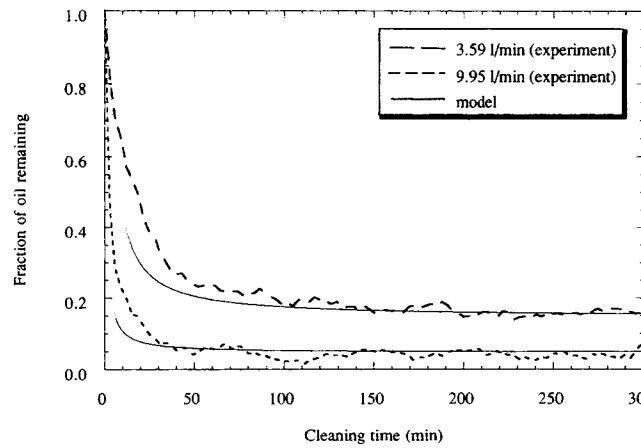

Figure 8. Effect of solvent flow rate on removal of Sunquench oil (fresh water, No. 63 cell, single coating).

residual amount of oil is held in the cavity by interfacial forces. When the flushant flow rate is increased, the higher shear rate is capable of removing some of the trapped oil, thereby reducing the amount of residual oil remaining at the end of the experiment.

Theoretical curves were obtained as explained in the previous section (Eqs. 12 and 14). It is important to emphasize that to generate the model predictions, only the value of α is required (as obtained from the asymptote at long times of the experimental curves). The comparison between the model and the experimental data indicates that the model overpredicts the cleaning rates at short times. This might be a consequence of the formation of interfacial instabilities, such as waves on the surface of the film. These waves might retard the removal by modifying the velocity profiles inside the film. The waves might also lead to eventual film rupture. It is not likely that the discrepancies between the model and the data are due to the motion of the contact line, since this would lead to experimental cleaning rates that are higher than those predicted by the model.

The hydrodynamics in the current decontamination experiments can be described in terms of core-annular flow (CAF), in which the annular fluid (oil) is removed by the core fluid (aqueous solution). Because of the difference in viscosities of the two fluids, instabilities exist at the interface between the two fluids. The stability of CAFs has been studied by a number of researchers (Hickox, 1971; Joseph et al., 1984; Preziosi et al., 1989; Hu and Joseph, 1989; Papageorgiou et al., 1990; Sangalli et al., 1995). Hickox (1971) demonstrated that, regardless of the Reynolds number value, the primary axisymmetric pipe flow is always unstable. Hu and Joseph (1989) identified three different kinds of instability: (1) the interfacial tension instability or capillary instability; (2) the interfacial friction instability due to the viscosity difference across the interface; and (3) the Reynolds stress instability. The Reynolds numbers in the current study are in the range of 7,257 to 20,091; hence, the interfacial tension instability can be neglected. Since the viscosity ratio between the two fluids (oil/water) is 132 for Sunquench and 64 for mineral oil, the interfacial friction instability should be taken into consideration. According to Hu and Joseph's (1989) criteria for this range of viscosity ratios and Reynolds numbers, the dominant instability in the current study is due to Reynolds stresses.

A study of the cleaning behavior as a function of metal surface treatment (Figure 9) indicates that the surface morphology has a significant effect on the removal rates and the final amount of oil remaining on the surface. The comparison is done at the low flow rate since at the higher flow rate the oil is taken away from the metal cavities more easily by the higher-velocity bulk flow and the surface roughness effect is reduced. The fractional residual oil α for the data in Figure 9 is 0.17 for the No. 63 tube and 0.05 for the No. 4 tube (see Table 3); this is equivalent to an oil film thickness of about 1.4×10^{-4} cm and 4.0×10^{-5} cm, respectively. These thicknesses are the same order of magnitude as the average roughness of the tubes ($\sim10^{-4}$ cm for No. 63 tube and $\sim10^{-5}$ cm for No. 4 tube). Residual oil in film removal experiments at relatively high surface roughness values has also been observed by Higdon (1985), Pozrikidis (1987), Yeckel et al. (1990), Mickaily et al. (1992), and Mickaily and Middleman (1993).

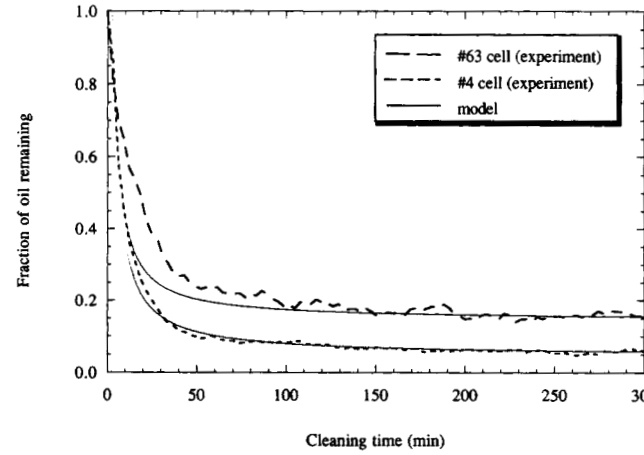

Figure 9. Effect of surface roughness on removal of Sunquench oil (fresh water, 3.59 L/min, single coating).

It is interesting to point out that the model adequately represents the cleaning behavior for the smoother tube (Figure 9). If interfacial waves are responsible for the discrepancies between the model and the experimental data, this result would indicate that interfacial instabilities are playing less of a role for the smooth tube. Therefore, it is possible that the instabilities are partly produced by perturbations in the velocity field within the film enhanced by wall roughness.

The effect of the surface morphology on the removal of contaminant residues is a function of the physical nature of the contaminant; in some cases the surface treatment may have a negligible effect on the removal of a residue. For example, in a previous study by our group, there was no difference in the rate and extent of the removal of solid calcium phosphate films from No. 4 and No. 63 stainless steel flow cells using aqueous solutions (Grant et al., 1996). In that study, the $Ca_3(PO_4)_2$ was removed from the tube surface by a combination of molecular dissolution and aggregate removal. Yiantsios and Karabelas (1994) developed a model to understand the removal process of solid residues (such as $CaCO_3$) by focusing on the structure and properties of the deposit layer. The deposit is modeled as a collection of roughness elements, which may represent polycrystalline agglomerates or colloidal particle aggregates. In contrast, during the removal of the oil residues the external solvent flow might cause fluid circulation in the cavities resulting in enhanced removal of the liquid contaminant. This has been reported by Chilukuri and Middleman (1982) in studies of liquids trapped in cavities.

Table 3. Experimental Values of Fractional Residual Oil

Contaminant	Q (L/min)	Surface Roughness	Surfactant Conc. (M)	α
Sunquench	3.59	No. 64	0	0.17
	9.95	No. 64	0	0.05
	3.59	No. 4	0	0.05
	3.59	No. 64	0.0024	0.075
	3.59	No. 64	0.0048	0.02
	3.59	No. 4	0.0024	0.017
Mineral Oil	3.59	No. 64	0	0.06

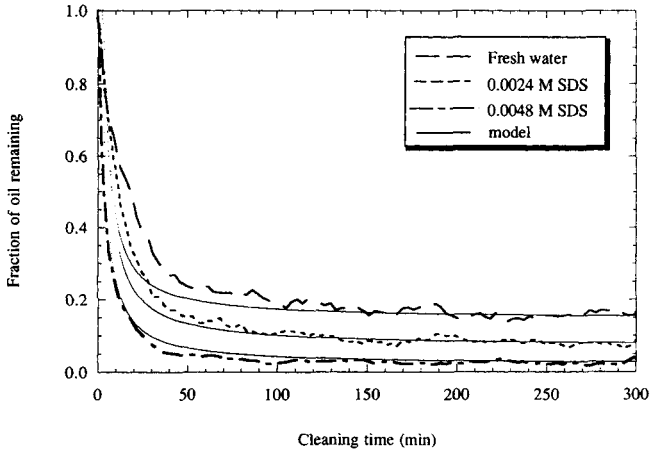

Figure 10. Effect of surfactant concentration on removal of Sunquench oil (No. 63 cell, 3.59 L/min, single coating).

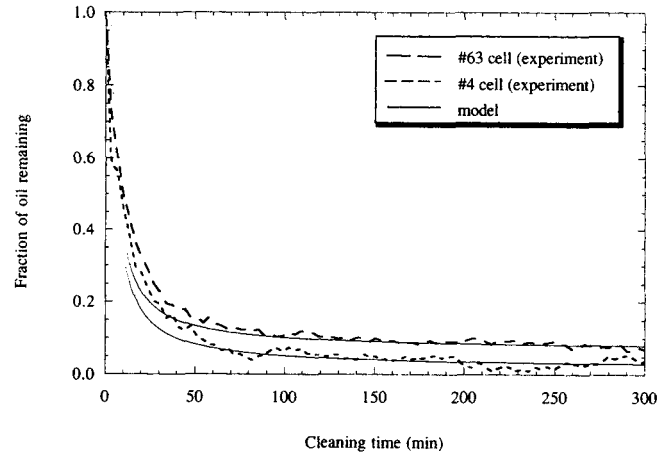

Figure 11. Effect of surface roughness on the removal of oil in presence of surfactant (0.0024 M SDS, 3.59 L/min, single coating, Sunquench).

Nonionic surfactants are often used to remove oily residues from solid surfaces (Beaudoin et al., 1995). Mickaily and Middleman (1993) speculated that in a tube cleaning process involving a surfactant, the hydrodynamics would dominate the removal in the thick-film regime (that is, at the beginning of the cleaning), whereas the surface interactions would become important as the oil film becomes thinner. The results in Figure 10 show that there is increased cleaning efficiency when SDS is present in the cleaning solution; the results also indicate that the rate and extent of cleaning is increased when the SDS concentration is increased from 2.4×10^{-3} M to 4.8×10^{-3} M.

There are three important mechanisms which have been identified in surfactant-based cleaning: roll-up (Fort et al., 1968; Aronson et al., 1983), emulsification (Raney and Miller, 1987; Raney et al., 1987; Cox et al., 1987), and solubilization (Shaeiwitz et al., 1981; Carroll, 1981). During a cleaning process involving a surfactant, the surfactant produces oil-enclosing micelles that are removed by the bulk flow. Even though throughout the cleaning process the removal of the oil is enhanced by the solubilization of the oil in the surfactant solutions, the main mechanism controlling the cleaning in our experiments is hydrodynamic, as proven by the removal rates in the absence of surfactant. An important conclusion from the results shown in Figure 10 (see also Table 3) is the decrease in fractional residual oil as the surfactant concentration is increased. This trend reflects a change in interface morphology as the cleaning process proceeds due to the presence of surfactant: at low oil contents, the removal process might be enhanced by roll up of oil beads on the surface and the cavities of the rough wall, induced by interfacial activity of the surfactant. Therefore, the presence of a surfactant partly overcomes the limitation on the ultimate cleaning imposed by surface roughness. Figure 11 shows how the surfactant is more effective at removing oil from the shallower cavities present in the No. 4 tube cell, as evidenced by the final extent of removal.

Figure 12 shows that mineral oil is easier to remove than Sunquench due to its lower viscosity. It is interesting to point out that the model better represents the results corresponding to mineral oil. Since the visocisty difference between the flushant (water) and the oil is lower for the mineral oil than for Sunquench, interfacial instabilities are less likely to develop and affect the cleaning process.

Conclusion

The removal of Sunquench 1042 and heavy mineral oil films from the inner side of a stainless steel tube cell using fresh water and SDS solutions has been studied. A novel radioactive tracer technique was used to determine the fraction of oil remaining as a function of cleaning time. The initial quick removal of the oils is associated with the shear stress at the oil/water interface when the oil film is still thick. As more oil is removed and the oil film becomes thinner, there exists an instability at the oil/water interface and the oil film breaks down. Towards the end of the decontamination run, oil left in the tube is trapped inside the cavities of the tube, remaining in place after the cleaning process ends.

Decontamination experiments conducted at different solution flow rates, surface roughnesses, SDS concentration, and

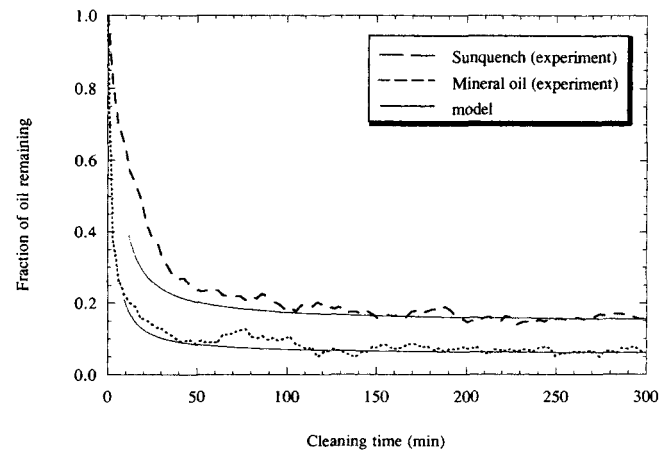

Figure 12. Comparison of the removal of two oils with different viscosities (fresh water, 3.59 L/min, No. 63 cell, single coating).

film viscosities indicate that the stainless steel surface morphology has a significant effect on the final extent of oil removed. The cleaning efficiency is significantly increased when SDS is used; moreover, the surfactant partly overcame the limitation on cleaning due to surface roughness.

The amount of residual oil remaining in the tube at the end of the cleaning process varies with flushant flow rate, surface roughness, and SDS concentration (see Table 3). Higher flow rates lead to lower levels of residual oil, that is, the residues are susceptible of being removed by an increase in the shear stress. An increase in surfactant concentration also leads to lower amounts of residual oil. This indicates that interfacial forces play a role at the end of the cleaning process.

Experimental results were compared with a hydrodynamic theory describing the removal of a liquid contaminant by an immiscible flushant. The deviation from the theory may be due to the surface roughness effect and the interfacial instabilities often associated with core-annular flow. The next phase of any hydrodynamic model to describe this removal process should consider the effect that interfacial instabilities have on the removal rates.

Acknowledgments

Financial support provided by a Cooperative Research Grant sponsored by the Advanced Cleaning Systems Group of The Dow Chemical Company, and by NSF grant No. CTS9500399 is gratefully acknowledged. The authors would like to thank Dr. Kuruvilla Verghese of the Dept. of Nuclear Engineering at North Carolina State University for his valuable discussion and suggestions in the development of the solid scintillation detection technique. We also thank Dr. Saad A. Khan and Ms. Joanna Roberts for the viscosity measurements.

Notation

t = flushing time
t^* = dimensionless flushing time variable
t = flushing time
t^* = dimensionless flushing time variable

Literature Cited

Aronson, M. P., M. L. Gum, and E. D. Goddard, "Behavior of Surfactant Mixtures in Model Oily-Soil Detergency Studies," *J. Amer. Oil Chem. Soc.*, **60**, 1333 (1983).

Beaudoin, S. P., R. G. Carbonell, and C. S. Grant, "Removal of Organic Films from Solid Surfaces Using Aqueous Solutions of Nonionic Surfactants: 1. Experiments," *Ind. Eng. Chem. Res.*, **34**, 3307 (1995).

Carroll, B. J., "The Kinetics of Solubilization of Nonpolar Oils by Nonionic Surfactant Solutions," *J. Colloid Interf. Sci.*, **79**, 126 (1981).

Chilukuri, R., and S. Middleman, "Circulation, Diffusion and Reaction within a Liquid Trapped in a Cavity," *Chem. Eng. Commun.*, **22**, 127 (1982).

Chowchury, J., and G. Ondrey, "Cleaning Goes High Tech," *Chem. Eng.*, 39 (1994).

Corrieu, G., "State-of-the Art of Cleaning Surfaces," *Fundamentals and Applications of Surface Phenomena Associated with Fouling and Cleaning in Food Processing*, Tylosand, Sweden, 90 (1981).

Cox, M. F., D. L. Smith, and G. L. Russell, "Surface Chemical Processes for Removal of Solid Sebum Soil," *J. Amer. Oil Chem. Soc.*, **64**, 273 (1987).

Fort, T. J., H. R. Billica, and T. H. Grindstaff, "Studies of Soiling and Detergency," *J. Amer. Oil Chem. Soc.*, **45**, 354 (1968).

Geankopolis, C., *Transport Processes and Unit Operations*, Prentice Hall (1993).

Grant, C. S., G. E. Webb, and Y. Jeon, "Calcium Phosphate Decontamination of Stainless Steel Surfaces," *AIChE J.*, **42**, 861 (1996).

Hickox, C. E., "Instability due to Viscosity and Density Stratification in Axisymmetric Pipe Flow," *Phys. Fluids*, **14**, 251 (1971).

Higdon, J. J. L., "Stokes Flow in Arbitrary 2-Dimensional Domains: Shear Flow over Ridges and Cavities," *J. Fluid Mech.*, **159**, 195 (1985).

Hu, H., and D. Joseph, "Lubricated Pipelining: Stability of Core-Annual Flow: II," *J. Fluid Mech.*, **205**, 359 (1989).

Jennings, W. J., "An Interpretative Review of Detergency for the Food Technologist," *Food Tech.*, **17**, 53 (1963).

Joseph, D., M. Renardy, and Y. Renardy, "Instability of the Flow of Two Immiscible Liquids with Different Viscosities in a Pipe," *J. Fluid Mech.*, **141**, 309 (1984).

Kulkarni, S. M., R. B. Maxcy, and R. C. Arnold, "Evaluation of Soil Desposition and Removal Processes: An Interpretative Review," *J. Dairy Sci.*, **58**, 1922 (1975).

Materials Performance, *NACE International*, p. 3 (Sept. 1994).

Mickaily, E. S., S. Middleman, and M. Allen, "Viscous Flow over Periodic Surfaces," *Chem. Eng. Commun.*, **117**, 401 (1992).

Mickaily, E. S., and S. Middleman, "Hydrodynamic Cleaning of a Viscous Film from the Inside of a Long Tube," *AIChE J.*, **39**, 885 (1993).

Papageorgiou, D. T., C. Maldarelli, and D. S. Rumschitzki, "Nonlinear Interfacial Stability of Core-annular Film Flows," *Phys. Fluids A*, **2**, 340 (1990).

Perka, A., C. S. Grant, and M. R. Overcash, "Waste Minimization in Batch Vessel Cleaning," *Chem. Eng. Commun.*, **119**, 167 (1993).

Plett, E. A., "Cleaning of Fouled Surfaces," *Fouling and Cleaning in Food Processing*, Univ. of Wisconsin, Madison, 288 (1985).

Pozrikidis, C., "Creeping Flow in a 2-D Channel," *J. Fluid Mech.*, **180**, 495 (1987).

Preziosi, L., K. Chen, and D. Joseph, "Lubricated Pipelining: Stability of Core-Annual Flow," *J. Fluid Mech.*, **201**, 323 (1989).

Raney, K. H., W. J. Benton, and C. A. Miller, "Optimum Detergency Conditions with Nonionic Surfactants. I. Ternary Water-Surfactant-Hydrocarbon Systems," *J. Colloid Interf. Sci.*, **117**, 282 (1987).

Raney, K. H., and C. A. Miller, "Optimum Detergency Conditions with Nonionic Surfactants: II. Effect of Hydrophobic Additives," *J. Colloid Interf. Sci.*, **119**, 539 (1987).

Royal Dutch/Shell Group of Companies, *The Petroleum Handbook*, Elsevier, New York (1983).

Sangalli, M., C. T. Gallagher, D. T. Leighton, H.-C. Chang, and M. J. McCready, "Finite-Amplitude Waves at the Interface between Fluids with Different Viscosity: Theory and Experiments," *Phys. Rev. Lett.*, **75**, 77 (1995).

Shaeiwitz, J. A., A. F.-C. Chan, E. L. Cussler, and D. F. Evans, "The Mechanism of Solubilization in Detergent Solutions," *J. Colloid Interf. Sci.*, **84**, 47 (1981).

Tsoulfanidis, N., *Measurement and Detection of Radiation*, Hemisphere Publishing Co., New York (1983).

van Os, N. M., J. R. Haak, and L. A. M. Rupert, *Physico-Chemical Properties of Selected Anionic, Cationic and Nonionic Surfactants*, Elsevier, Amsterdam, The Netherlands, p. 16 (1993).

Wennerberg, J., "Observations on the Behaviour of Fouling and Cleaning in Industrial Processes," *Fundamentals and Applications of Surface Phenomena Associated with Fouling and Cleaning in Food Processing*, Tylosand, Sweden, 76 (1981).

Yeckel, A., S. Middleman, and L. Klumb, "The Removal of Thin Liquid Films from Periodically Grooved Surfaces by an Impinging Jet," *Chem. Eng. Comm.*, **96**, 69 (1990).

Yiantsios, S. G., and A. J. Karabelas, "Fouling of Tube Surfaces: Modeling of Removal Kinetics," *AIChE J.*, **40**, 1804 (1994).

Manuscript received Sept. 11, 1995, and revision received June 21, 1996.